Low-threshold continuous-wave operation of quantum-cascade lasers grown by metalorganic vapor phase epitaxy

Permanent link

http://nrs.harvard.edu/urn-3:HUL.InstRepos:41371374

Low-threshold continuous-wave operation of quantum-cascade lasers grown by metalorganic vapor phase epitaxy

Mariano Troccoli[a)]
Division of Engineering and Applied Sciences, Harvard University, Cambridge, Massachusetts 02138

David Bour, Scott Corzine, Gloria Höfler, Ashish Tandon, and Dan Mars
Agilent Labs, 3500 Deer Creek Road, Palo Alto, California 94304

David J. Smith
Department of Physics and Astronomy and Center for Solid State Science, Arizona State University, Tempe, Arizona 85287-1704

Laurent Diehl and Federico Capasso
Division of Engineering and Applied Sciences, Harvard University, Cambridge, Massachusetts 02138

We report on the realization of InGaAs/InAlAs quantum-cascade lasers grown by metalorganic vapor phase epitaxy operating in continuous wave with low-threshold current densities at temperatures as high as 188 K. Threshold current densities of 950 A/cm^2 and output powers of 125 mW are measured at 80 K, while 3 mW of continuous output power are measured at 180 K, with a threshold of 2.5 kA/cm^2. In pulsed mode, peak output powers of more than 0.4 W were obtained at 80 K and of 160 mW at 300 K with thresholds of 700 A/cm^2 and 2.75 kA/cm^2, respectively. © *2004 American Institute of Physics.* [DOI: 10.1063/1.1834715]

Quantum cascade (QC) lasers[1,2] have been grown so far preferentially by molecular beam epitaxy (MBE), a growth technique that has brought very promising results for the applications of these mid- to far-infrared sources. Room temperature (RT), cw operation has been achieved[3] and recent improvements have demonstrated high powers and low thresholds for RT operation.[4] However, an important step in the development of quantum cascade laser technology is the capability to grow high-quality material by metalorganic vapor phase epitaxy (MOVPE), enabling low cost and high yield production of lasers working at room temperature with high powers. MOVPE-grown quantum cascade lasers have been operated in pulsed mode and had high thresholds and low powers at RT.[5,6] This letter presents the cw operation of MOVPE-grown quantum-cascade lasers up to temperatures as high as 188 K and delivering more than 125 mW of output power at 80 K, with threshold current densities of 750 A/cm^2. RT ($T=300$ K) operation is also demonstrated in pulsed mode, with peak powers of 160 mW and thresholds of 2.75 kA/cm^2, while peak powers of 0.45 W are obtained at 80 K.

We have grown a 30-stage AlInAs/GaInAs QC laser structure lattice matched to the InP substrate, similar to that described by Gmachl *et al.*,[7] by conventional, low-pressure (76 Torr) MOVPE. This laser design provides state-of-the-art performance and has been used in many sensing applications.[8] Our Thomas Swan reactor incorporates a purged and pressure-balanced switching manifold and a close-spaced showerhead injector. Similar to the conditions employed by Green *et al.*,[6] the growth rate for the quantum-cascade active region was set very low (0.1 nm/s), and 5 s growth stops were employed at all interfaces. The remainder of the structure was grown at approximately five times this rate. Precursors include trimethylindium, triethylgallium (for the slow-grown QC structure only), trimethylgallium (for the

InGaAs separate confinement heterostructure), trimethylaluminum, arsine, phosphine, and disilane (0.01% in H$_2$) for *n*-type doping. The samples were grown at a temperature of 650 °C (calibrated by the eutectic temperature of Al–Si) on (001)-oriented InP:S ($n=3\times10^{18}$ cm^{-3}) substrates. To avoid excessive free-carrier loss associated with the high doping in the substrate, a relatively thick (3 μm) low-doped *n*-type InP:Si ($n=2\times10^{17}$ cm^{-3}) cladding layer was grown before the 0.45-μm-thick, $n=5\times10^{16}$ cm^{-3} doped, InGaAs waveguide core layers that enclose the quantum cascade active region. Likewise, the InP upper cladding layer is similarly thick, to minimize the loss arising from the top layer, highly doped for plasmon-enhanced confinement of the laser mode (500 nm InP:Si with $n=5\times10^{18}$ cm^{-3}), and from the top metal contact. The ability to grow such thick InP cladding layers is a primary advantage of MOVPE. The quantum-cascade active region is nominally identical to that reported by Gmachl *et al.*[7] To reduce the series resistance, the interfaces between the InGaAs waveguide core layers and the InP cladding layers comprise 30 nm step-graded InGaAsP.

The measured (004) double-crystal x-ray diffraction spectrum of the QC laser wafer is shown in Fig. 1(a), in comparison to the simulated spectrum (bottom). Satellite reflections are clearly visible, indicating the presence of a periodic structure. The spacing of the satellites indicates a periodicity of about 42 nm, corresponding to the thickness of each QC stage. This is slightly thinner than the designed stage thickness of 44.3 nm. This difference could be an indication of a systematic error, where each layer forming the QC stack is about 5% too thin. To further investigate the interface quality, we performed transmission electron microscopy (TEM) of the active region as shown in Fig. 1(b). Cross-section samples were prepared for TEM examination by standard mechanical polishing, dimpling, and final ion-beam milling to perforation. Observations were made with a JEM-4000EX high-resolution electron microscope operated at 400 keV. Samples were viewed in bright-field mode at or

---
[a)]Electronic mail: troccoli@deas.harvard.edu

Appl. Phys. Lett., Vol. 85, No. 24, 13 December 2004
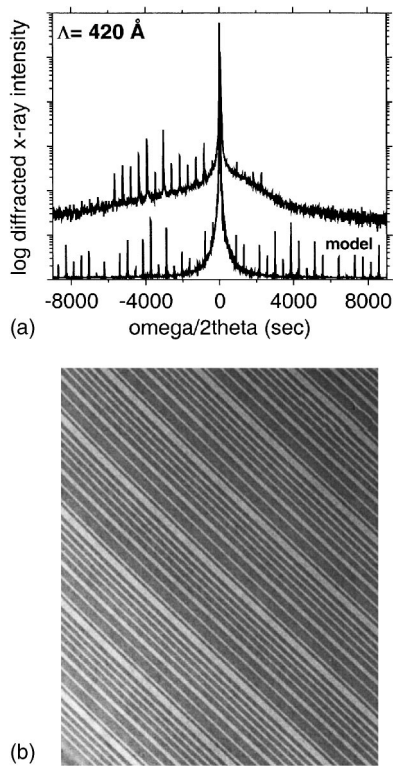
Troccoli *et al.*   5843

(a)

(b)

FIG. 1. (a) Double-crystal x-ray diffraction spectra (measured-top, simulated-bottom) of the measured QC laser wafer and (b) TEM bright-field image of a section of the active region. $Ga_{0.47}In_{0.53}As$ layers are dark and $Al_{0.48}In_{0.52}As$ layers are light.
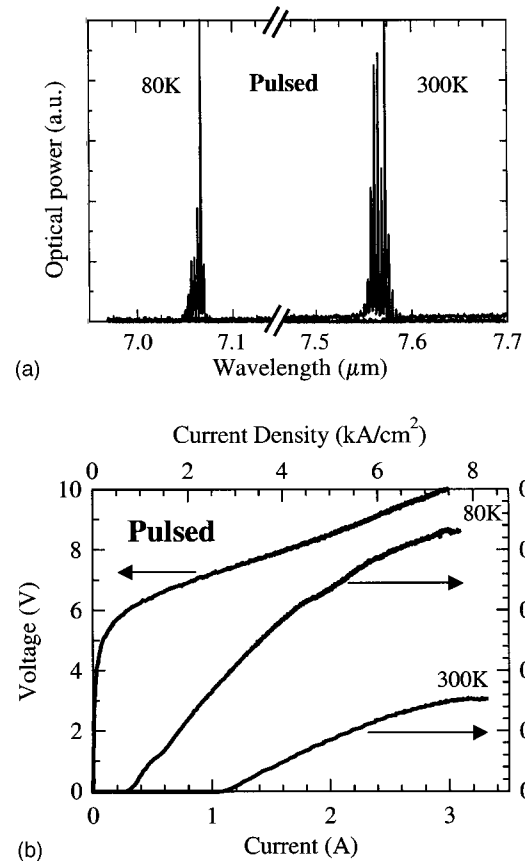

(a)

(b)

FIG. 2. (a) Pulsed operation emission spectra from the QC laser at temperatures of 80 and 300 K and currents of 0.3 and 1.1 A, respectively. The Fabry–Perot modes are clearly distinguishable. (b) Voltage–current ($I-V$) and light–current ($L-I$) characteristics of the same laser operated in pulsed mode with a duty cycle of 0.05%. The $I-V$ shown is the one measured at 80 K together with the corresponding $L-I$, while only the $L-I$ characteristic is shown for the room temperature operation for clarity reasons.

close to the common [110]-type projection. Clearest differentiation between the various layers was achieved using a small objective aperture. The TEM image confirms the good quality of the interface abruptness that can be achieved by MOVPE and the shorter than expected periodicity of the active region.

The lasers were fabricated as ridge waveguide structures, wet-etched down to the lower InP layer, and with a 350-nm-thick Si_3N_4 insulating layer deposited on the lateral walls of the waveguide. A Ti(30 nm)/Au(350 nm) top contact and a Ge(12 nm)/Au(27 nm)/Ag(50 nm)/Au(250 nm) back contact were deposited and the devices were indium soldered from the substrate side onto a Ni/Au-plated copper block. The samples were then mounted in a liquid-N_2 flow cryostat for the low-temperature measurements.

Figure 2(a) shows the spectral measurements at 80 and 300 K for lasers operated in pulsed mode, with 100 ns current pulses at a repetition rate of 11 kHz. A Fourier-transform infrared spectrometer equipped with a deuterated triglycine sulfate detector was employed for these measurements. The room-temperature emission is at 7.6 μm, blue-shifted by 6% relative to the original design at 8.1 μm.[7] This is possibly explained by the x-ray and TEM measurements that showed a 5% reduction in the layer thickness, which would likely induce a shift of the emission toward higher energies. Further calibration of the growth procedure should easily correct for this discrepancy. The voltage–current and output power–current characteristics for the lasers operated in pulsed mode at 80 and 300 K are also shown in Fig. 2(b). At the lowest temperature, peak powers of 0.45 W are attained, with threshold currents of 300 mA (700 A/cm²), while at 300 K the maximum power output is of 160 mW with thresholds of 1.1 A (2.75 kA/cm²). The power was

measured with a calibrated room temperature HgCdTe photodetector.

The cw-operation data are shown in Figs. 3 and 4. The spectra acquired from a cw-operated 14-μm-wide laser close to threshold are shown in Fig. 3(a). Lasing from 80 to 180 K is observed and in most cases the spectra show single mode operation with almost 30 dB of side mode suppression ratio [see Fig. 3(a), inset]. Well above threshold the spectra become multimode, as shown in Fig. 3(b), where typical emission spectra acquired just above threshold ($I=350$ mA) and at about twice the threshold current ($I=600$ mA) are shown together with the corresponding light–current characteristic of the device measured at a heat sink temperature of 80 K.

The cw power–current and voltage–current characteristics are displayed in Fig. 4(a). At 80 K, threshold currents of 0.3 A (950 A/cm²) and a slope efficiency of 135 mW/A have been recorded, and cw operation is observed up to 180 K with thresholds of 0.9 A and a maximum power of 3 mW. By coating the back facet of this same sample, we were able to reduce the threshold current by 25% and increase continuous wave operation up to 188 K. From wider laser stripes (20 μm wide, 2 mm long) higher powers of 125 mW were obtained at 80 K with a slope efficiency of 285 mW/A, but cw operation was observed only up to 140 K due to the larger amount of heat that must be dissipated [Fig. 4(b)]. The differential resistance value derived from the cw voltage–current measurements at 80 K is plotted
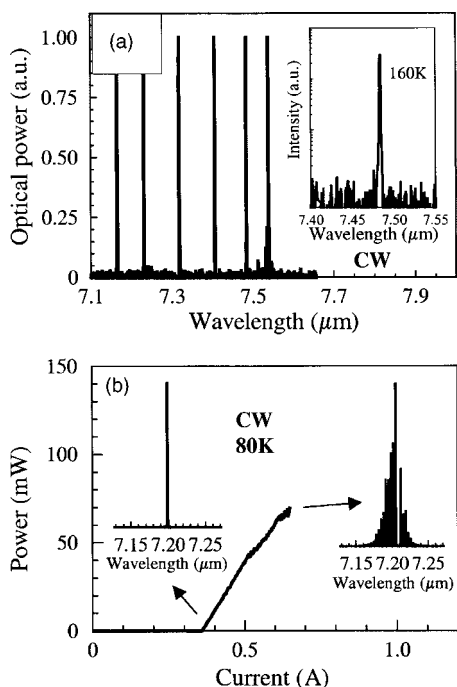
FIG. 3. (a) Normalized continuous wave spectra measured from a 14-μm-wide laser stripe at temperatures of (from left to right) 80, 100, 120, 140, 160, 180 K and currents of 0.35, 0.36, 0.4, 0.5, 0.7, and 0.95 A, respectively. Inset: Logarithmic scale plot of the 160 K spectrum, showing a side mode suppression of almost 30 dB. (b) Comparison of typical cw emission spectra at currents close to threshold (I=0.35 A, left side) and at about twice the threshold current (I=0.6 A, right side), shown together with the relative light–current characteristic for a device measured at 80 K.

in the inset of Fig. 4(a), and it can be noticed that at around 0.3 A, corresponding to the laser threshold current, there is a sudden lowering of the differential resistance. This effect is commonly observed in MBE-grown QC lasers as well and is due to the change in lifetime of the laser transition at threshold.[9]

Devices fabricated from wafers grown in different conditions were also characterized. We compared the data shown here with those obtained from samples grown at higher rates (0.5 instead of 0.1 nm/s) and with samples grown at a low rate but without growth stops at the interface between different materials. The performances in both cases were not as good as the ones presented here, with an increase of 30% in the threshold and a decrease of 50% in the slope efficiency for the samples without growth stops and a low growth rate, and an increase of 60% in threshold for the sample grown at higher rate.[10]

In conclusion, we presented emission data from MOVPE-grown QC lasers that demonstrate performances that start to be competitive with state-of-the-art MBE-grown devices, an encouraging step toward a wider application of this technology. The most important advantages of the application of MOVPE technology to the growth of QC lasers reside in the possibility of growing very thick layers (typically cladding and burying layers) and in the possibility to grow at high temperatures, thus promoting smoother surfaces. Moreover, MOVPE is typically more stable over long growth times (typical of QC lasers) and allows one to grow continuously graded semiconductor alloys. Finally, higher growth rates are possible, but it still remains to be proven that they are viable for the production of QC lasers. The main drawback of MOVPE with respect to MBE is that the
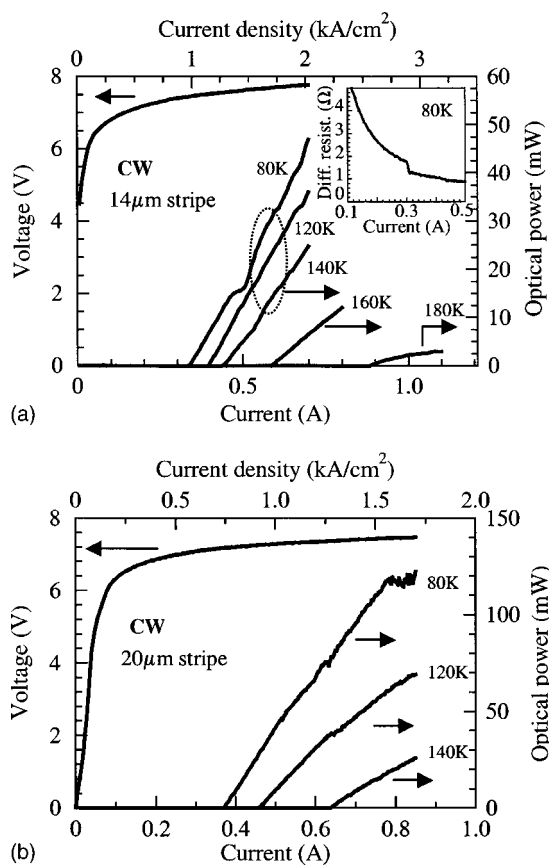

FIG. 4. (a) cw I–V and optical power-current (L–I) characteristics of a 14-μm-wide, 2-mm-long, laser stripe measured at temperatures of 80 K (I–V and leftmost L–I), 120, 140, 160, and 180 K, from left to right. Inset: differential resistance derived from the I–V curve, where a dip is clearly visible at the current corresponding to the laser threshold at 80 K. (b) cw I–V and L–I measurements for a 20-μm-wide, 2-mm-long laser ridge waveguide. The L–I curves were measured at temperatures of (from left to right): 80, 120, 140 K, while the I–V shown is the one recorded at 80 K.

formation of abrupt interfaces can be more challenging, a characteristic that may be important but not obviously related to the laser performances. The optimization of device packaging by use of InP re-growth and thick gold plating on the top contact combined with mounting the device epitaxial-side down on the heat sink would improve the performances even further and bring the lasers close to room temperature continuous operation.

[1]F. Capasso, R. Paiella, R. Martini, R. Colombelli, C. Gmachl, T. L. Myers, M. S. Taubman, R. M. Williams, C. G. Bethea, K. Unterrainer, H. Y. Hwang, D. L. Sivco, A. Y. Cho, A. M. Sergent, H. C. Liu, and E. A. Whittaker, IEEE J. Quantum Electron. **38**, 511 (2002).
[2]F. Capasso, C. Gmachl, D. L. Sivco, and A. Y. Cho, Phys. Today **55**, 34 (2002).
[3]M. Beck, D. Hofstetter, T. Aellen, J. Faist, U. Oesterle, M. Ilegems, E. Gini, and H. Melchior, Science **295**, 301 (2002).
[4]A. Evans, J. S. Yu, J. David, L. Doris, K. Mi, S. Slivken, and M. Razeghi, Appl. Phys. Lett. **84**, 314 (2004).
[5]J. S. Roberts, R. P. Green, L. R. Wilson, E. A. Zibik, D. G. Revin, J. W. Cockburn, and R. J. Airey, Appl. Phys. Lett. **82**, 4221 (2003).
[6]R. P. Green, A. Krysa, J. S. Roberts, D. G. Revin, L. R. Wilson, E. A. Zibik, W. H. Ng, and J. W. Cockburn, Appl. Phys. Lett. **83**, 1921 (2003).
[7]C. Gmachl, A. Tredicucci, F. Capasso, A. L. Hutchinson, D. L. Sivco, J. N. Baillargeon, and A. Y. Cho, Appl. Phys. Lett. **72**, 3130 (1998).
[8]A. A. Kosterev and F. K. Tittel, IEEE J. Quantum Electron. **38**, 582 (2002).
[9]C. Sirtori, F. Capasso, J. Faist, A. L. Hutchinson, D. L. Sivco, and A. Y. Cho, IEEE J. Quantum Electron. **34**, 1722 (1998).
[10]M. Troccoli, O. Assayag, L. Diehl, D. Bour, S. Corzine, G. Höfler, A. Tandon, D. Mars, and F. Capasso (unpublished).